Electronic Supplementary Information (ESI)

Spatial decoupling of macrocyclic metal-organic complexes from a metal support: a 4-fluorothiophenol self-assembled monolayer as thermally removable spacer

Peter S. Deimel[1], Peter Feulner[1], Johannes V. Barth[1], and Francesco Allegretti[1*]

[1]Physics Department E20, Technical University of Munich, 85748 Garching, Germany

[*] Corresponding author: francesco.allegretti@ph.tum.de

C 1*s* XP spectrum of the 4-FTP SAM on Ag(111)

Fig. S1 shows the C 1*s* XP spectrum associated with the S 2*p* spectrum labelled 1 in Fig. 3a of the main manuscript, corresponding to a saturated monolayer of 4-FTP on Ag(111) and recorded at a sample temperature of 90 K. The fitting has been performed using the FitXPS software[1], with three Gaussian peaks constrained to the same full width at half maximum (FWHM) and superimposed on a linear background.

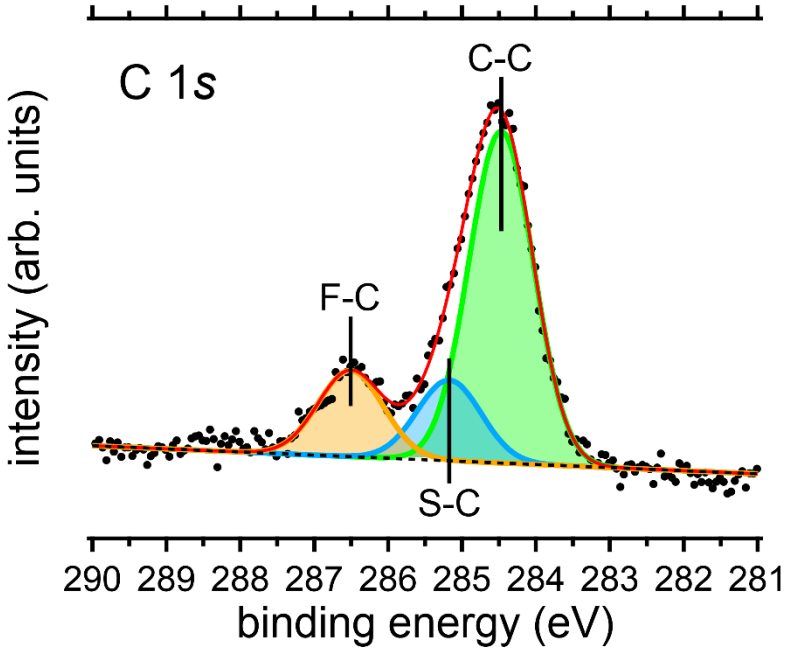

Fig. S1 Normal emission (NE) C 1*s* XP spectrum of the saturated monolayer of 4-FTP, deposited on the Ag(111) surface at 300 K and corresponding to the S 2*p* XP spectrum 1 in Fig. 3a. This C 1*s* spectrum has been recorded subsequent to spectrum 1 in Fig. 3a, at the same conditions and with the same measurement settings.

The dominant peak at 284.5 eV (C-C) is ascribed to the four carbon atoms that are each bound to two other carbon atoms of the aromatic ring. The second feature at 285.2 eV (S-C) is assigned to the carbon species in the intact C-S moiety and the third, more clearly resolved component at 286.5 eV (F-C) is attributed to the carbon atom bound to the fluorine end group. Importantly, the determined binding energy positions of the ascribed peaks are in excellent agreement with the fitting results for the 4-FTP SAM

on Ni(111) by Blobner *et al.*[2]. Furthermore, the area ratio for the three chemically distinct components is 1 (C-C) : 0.24 (S-C) : 0.26 (F-C), which nicely matches the stoichiometric ratio of 4 (C-C) : 1 (S-C) : 1 (F-C) expected for 4-FTP. This result confirms that the 4-FTP molecules within the SAM are intact, and specifically, that the integrity of the C-S bond is preserved upon adsorption, as stated in the main manuscript.

Fe $2p_{3/2}$ XP spectra of FePc on Ag(111) before and after exposure to 4-FTP

Fig. S2 shows the Fe $2p_{3/2}$ XP spectra of an FePc coverage slightly lower than the densest monolayer packing on Ag(111), before (spectrum 1, blue) and after (spectrum 2, red) deposition of 4-FTP at 300 K. As stated in the text, no considerable modification of the Fe $2p_{3/2}$ line shape is observed between spectrum 1 and 2 (prior to and after 4-FTP exposure). Both spectra resemble the shape of the reference monolayer of FePc on Ag(111) shown in spectrum 3. This suggests that the 4-FTP molecules, co-adsorbed in the form of a Ag-bound thiolate, do not coordinate to the Fe centres.

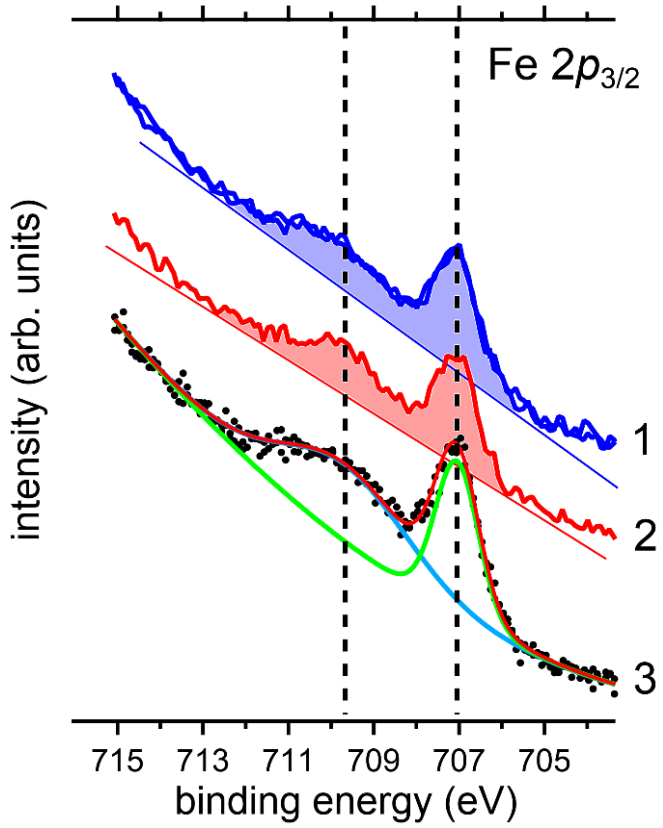

Fig. S2 Grazing emission (GE) Fe $2p_{3/2}$ XP spectra of (1) an FePc coverage on Ag(111) slightly lower than the densest monolayer (T_{meas} = 300 K), (2) the system in (1) after 4-FTP exposure at 300 K (T_{meas} = 300 K) and (3) the reference monolayer of FePc on Ag(111) shown in spectrum 5 of Fig. 5a (T_{meas} = 90 K). Note that spectrum 1 corresponds to the system of the S 2*p* (GE) XP spectrum 1 of Fig. 4c and, similarly, spectrum 2 corresponds to the system investigated in spectrum 2 of Fig. 4c. The straight lines and shaded areas in spectra 1 and 2 are arbitrarily drawn to facilitate the visual comparison.

S 2*p* XP spectra of FePc/4-FTP/Ag(111) after annealing to 300 K

Fig. S3 displays the fitted S 2*p* spectra for FePc deposited onto the 4-FTP SAM on Ag(111) at 90 K, followed by annealing to 300 K (spectra 3, 3' and 3''), and for FePc deposited onto 4-FTP/Ag(111) directly at 300 K (spectrum 3'''). The spectrum of the 4-FTP SAM on Ag(111) (spectrum 1) serves as reference for the Ag-bonded thiolate species of 4-FTP and, as spectra 3 and 3', has already been shown in Fig 6a of the main manuscript. In contrast to spectrum 3', for the fitting of spectra 3, 3'' and 3''' an additional thiolate species (with peak positions constrained to 161.75 eV and 162.95 eV, respectively, for the S $2p_{3/2}$ and $2p_{1/2}$ components) is introduced to obtain a good fit. By comparison with the dominant S 2*p* features at 162.3 eV and 163.5 eV, evolving after annealing the systems to 300 K (or by depositing FePc onto 4-FTP/Ag(111) directly at 300 K), this indicates that some of the 4-FTP remains directly bound to the Ag(111) surface as thiolate. We ascribe the presence of this thiolate species to the deposition of less than a full layer coverage of FePc on Ag(111). The latter would be needed to completely remove 4-FTP from the Ag(111) surface as in spectrum 3'. Note also that spectrum 3 corresponds to the LEED pattern of Fig. 5d (main manuscript), corroborating the assumption that the remaining Ag-bound thiolate species is compressed to a denser phase. Fitting has been performed with the FitXPS software[1], using two S 2*p* spin-orbit doublets of fixed energy splitting (1.2 eV), fixed intensity ratio and similar FWHM, and a linear background.

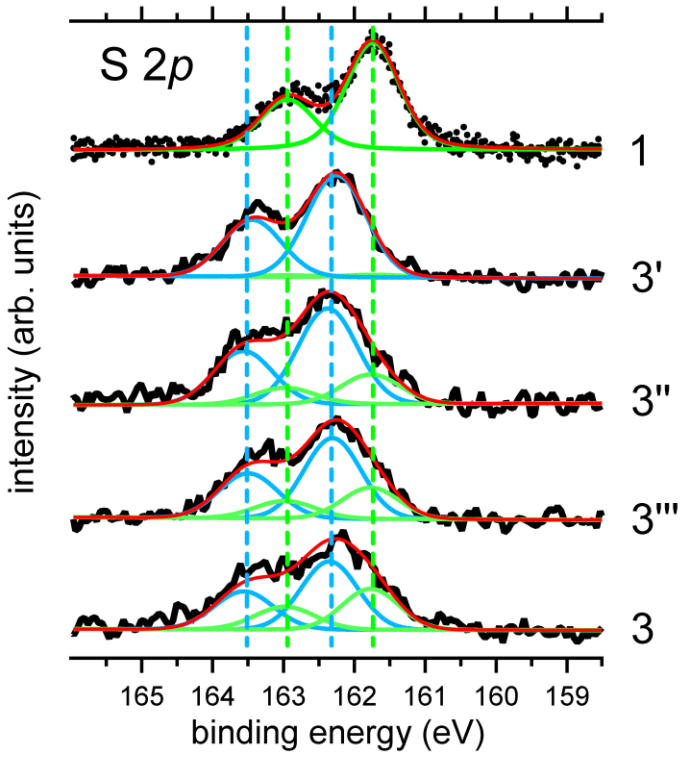

Fig. S3 S 2*p* (NE) XP spectra of (1) 4-FTP SAM on Ag(111), (3)(3′)(3′′) FePc deposited onto the 4-FTP SAM on Ag(111) at 90 K, followed by annealing to 300 K, and (3′′′) FePc deposited onto the 4-FTP SAM on Ag(111) at 300 K. Spectrum 3′′′ has been recorded at 300 K, all other spectra have been recorded at 90 K. Spectrum 3 is recorded on the same system as the LEED pattern in Fig. 5d of the main manuscript.

C 1*s* XP spectra of the thermal evolution of FePc/4-FTP/Ag(111)

Fig. S4 shows the C 1*s* (NE) XP spectra for the 4-FTP SAM on Ag(111) (spectrum 1), the FePc monolayer on Ag(111) (spectrum 2), a FePc layer deposited onto the 4-FTP SAM on Ag(111) at 90 K (spectrum 3), and the system of spectrum 3 after annealing to 300 K (spectrum 4). Importantly, in spectrum 4 the C 1*s* feature at around 286.5 eV, ascribed to the 4-FTP carbon atom bound to fluorine (cf. Fig. S1, F-C), is restored. This corroborates the conclusion that (from 3 to 4) 4-FTP is displaced from the Ag(111) surface moving on top of the FePc layer (cf. schematic 4), preventing attenuation of the associated C 1*s* features by FePc. In contrast, the 4-FTP related feature at ~286.5 eV is attenuated by the FePc overlayer in spectrum 3. The C 1*s* data thus support the intercalation of FePc, as stated in the main manuscript.

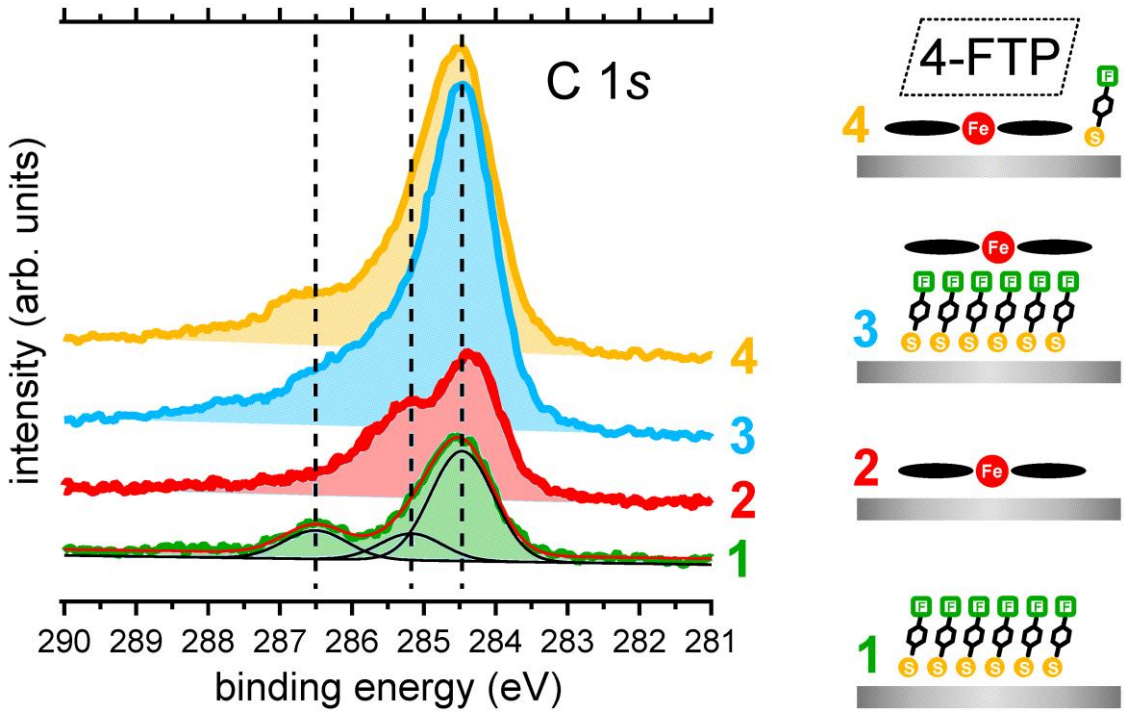

Fig. S4 C 1*s* (NE) XP spectra of (1) the 4-FTP SAM on Ag(111), (2) the saturated FePc monolayer on Ag(111) and (3) FePc deposited onto the 4-FTP SAM at 90 K, followed by (4) annealing to 300 K. All spectra were recorded at 90 K. Spectrum 1, including the fitted peaks, corresponds to the C 1*s* spectrum in Fig. S1. Suggested (explanatory) overlayer morphologies are sketched on the right.

S 2*p* XP spectra of the thermal evolution of FePc/4-FTP/Ag(111)

Fig. S5a,b shows the S 2*p* (NE) XP spectra for the 4-FTP SAM on Ag(111) (green spectra, sketch 1), FePc deposited onto the 4-FTP SAM on Ag(111) at 90 K (light-blue spectra, sketch 3), and the latter after having been annealed to 300 K (light-orange spectra, sketch 4). After deposition of FePc, the S 2*p* signal gets slightly attenuated, due to the FePc molecules sitting on top of the SAM (sketch 3). However, after annealing the systems to 300 K, the pronounced blue shift of the S 2*p* features is accompanied by an overall increase of the corresponding S 2*p* signal intensity. The gain in S 2*p* signal intensity supports the assumption that FePc penetrates the SAM at temperatures above 175 K, coming into contact with the Ag(111) surface and resulting in the inverted layer stacking illustrated in sketch 4. The ratio of the integrated areas under the S 2*p* spectra of Fig. S5a,b amounts to roughly 1 : 0.9 : 1.1 (system 1 : system 3 : system 4), normalized against the S 2*p* intensity of the 4-FTP SAM on Ag(111) (sketch 1).

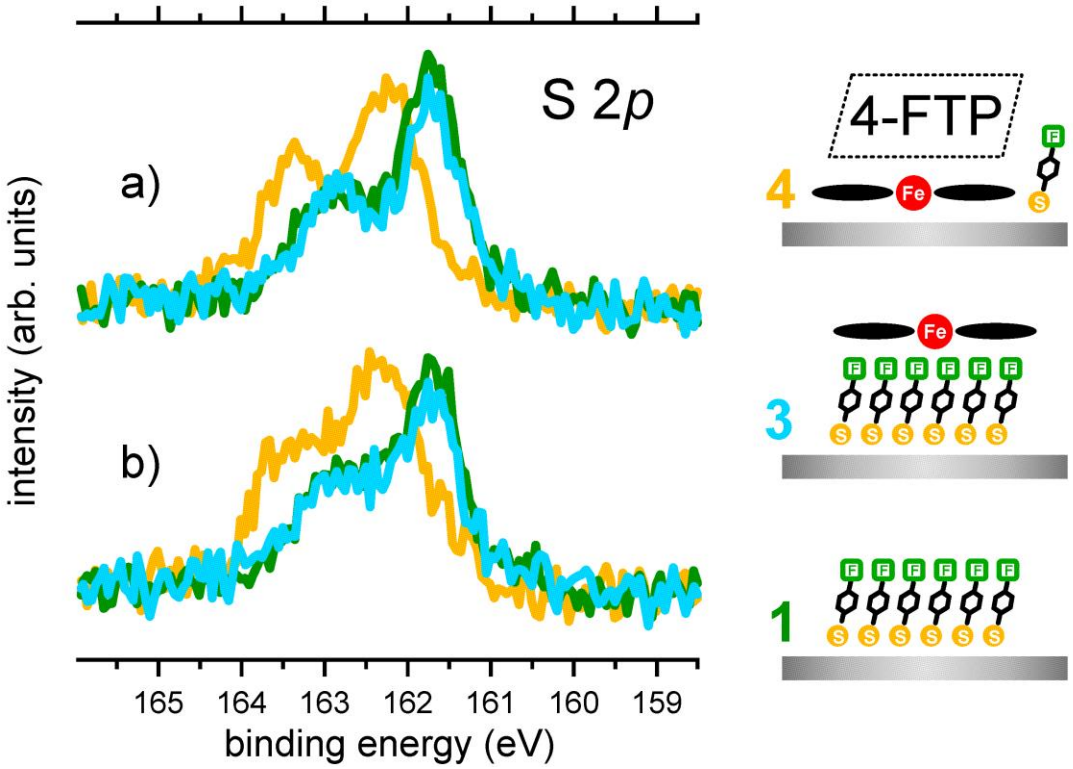

Fig. S5 S 2*p* (NE) XP spectra of the 4-FTP SAM on Ag(111) (green spectra), FePc deposited onto the 4-FTP SAM at 90 K (light-blue spectra), and of the latter system after annealing to 300 K (light-orange spectra). The two sets of data correspond to two different preparations. All spectra were recorded at a sample temperature of 90 K. Suggested overlayer morphologies are sketched on the right.

TPD spectra of the 4-FTP SAM on Ag(111), with and without FePc or Ru(CO)TPP deposited on top

Fig. S6 shows the TPD spectra for the various systems of Fig. 9a (main manuscript), with addition of the spectra for m/z = 127 and 128. It can be observed that the signal at m/z = 128 (the parent ion of the intact 4-FTP) exhibits a striking similarity with the signal at m/z = 108. In addition, the signal at m/z = 127 (ascribed to the thiolate radical, a half-split disulphide or a doubly ionized disulphide) behaves very similarly to the signal at m/z = 83. This corroborates the assumption that the mass signals m/z = 108 and 83 serve as distinctive measure for the desorption of the thiol and the thiolate-related species (the thiolate radical or disulphide species), respectively. Considering the nature of the latter, direct desorption as thiolate radical was observed to be dominant over disulphide desorption for low density structures of hexanethiol on Au(111)[3, 4], specifically stressing the impact of molecular density, associated steric constraints, surface structure and molecule-substrate interactions on the actual desorption products[5, 6].

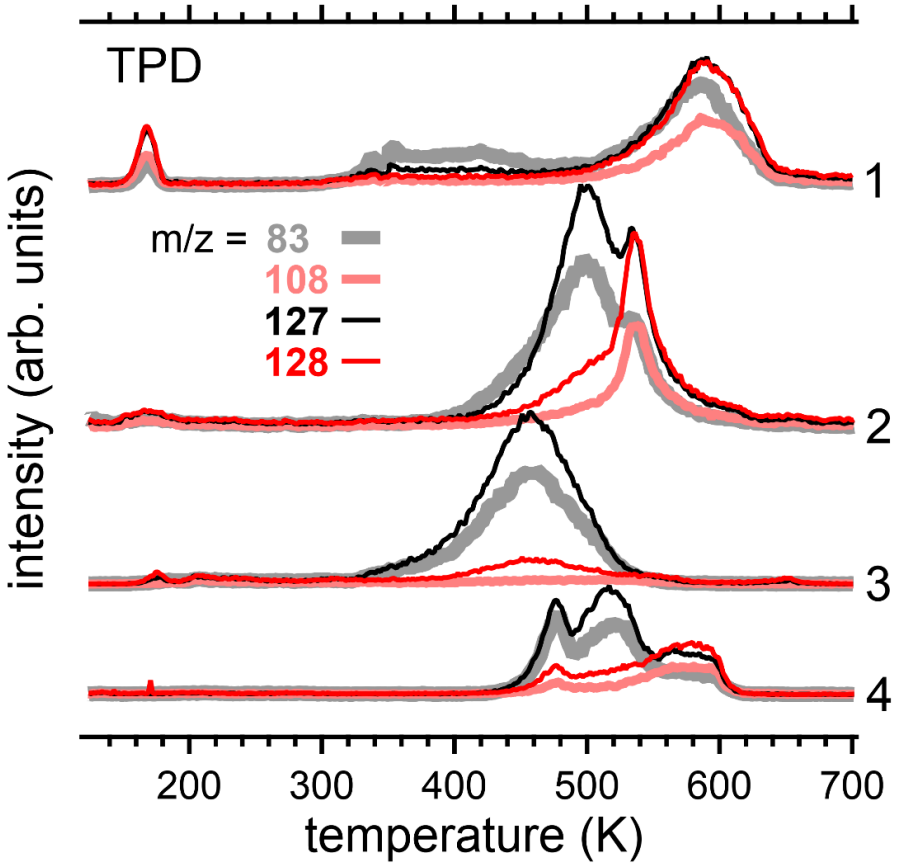

Fig. S6 TPD spectra for m/z = 83 (grey), m/z = 108 (light red), m/z = 127 (black) and m/z = 128 (red) of (1) 4-FTP SAM on Ag(111), (2) FePc on the 4-FTP SAM/Ag(111), (3) higher coverage of FePc (as compared to (2)) on the 4-FTP SAM/Ag(111) and (4) Ru(CO)TPP on the 4-FTP SAM/Ag(111). The TPD spectra have been recorded in the range 120 – 700 K with a heating rate of 0.5 K/s.

References

1. D. L. Adams and J. N. Andersen, FitXPS Version 2.12, University of Aarhus, Denmark.
2. F. Blobner, P. N. Abufager, R. Han, J. Bauer, D. A. Duncan, R. J. Maurer, K. Reuter, P. Feulner and F. Allegretti, *J. Phys. Chem. C*, 2015, **119**, 15455-15468.
3. H. Kondoh, C. Kodama and H. Nozoye, *J. Phys. Chem. B*, 1998, **102**, 2310-2312.
4. H. Kondoh, C. Kodama, H. Sumida and H. Nozoye, *J. Chem. Phys.*, 1999, **111**, 1175-1184.
5. T. Hayashi, K. Wakamatsu, E. Ito and M. Hara, *J. Phys. Chem. C*, 2009, **113**, 18795-18799.
6. E. Ito, H. Ito, H. Kang, T. Hayashi, M. Hara and J. Noh, *J. Phys. Chem. C*, 2012, **116**, 17586-17593.